An ERPNS Technology Based on OFDR for Accurate Arm-Length Difference Measurement of Optical Fiber Interferometer Under Dynamic Environment

Luwei Shuai, Lei Ye, and Qing Ye

***Abstract*—Accurate measurement of interferometer arm-length difference is very important in the application fields such as fiber optic hydrophones. However, the interferometer is very sensitive to the environmental vibration and noise, which affects the accuracy of the interferometer measurement. A novel environmental random phase noise separation (ERPNS) technology is proposed to effectively reduce optical frequency domain reflectometer (OFDR)'s sensitivity to environmental vibration for the measurement of the fiber interferometer. A set of optical paths based on dual-laser coherent detection technology and the related ERPNS algorithm was developed to extract the environmental phase noise from the measurement data. The OFDR's sensitivity to vibration is decreased by ∼60 dB in theory and a measurement accuracy better than 0.05 mm for the static arm length difference of 74.51902 m in different dynamic environment is achieved experimentally, with 56 μm of spatial resolution in the maximum detectable distance of about 75 m.**

***Index Terms*—OFDR, arm-length difference, ERPNS, dynamic environment.**

I. Introduction

THE fiber optic hydrophones based on Michelson interferometer have been widely used in the field of underwater acoustic sensing due to its excellent sensitivity, dynamic range and large-scale multiplexing ability [1], [2], [3], [4]. For the interferometric fiber-optic hydrophone, the laser phase noise is a fundamental noise source, and the level of phase noise associated with the laser frequency noise is proportional to the optical path difference in the interferometer and this can be eliminated by path matching the interferometer [5]. Therefore, when the hydrophones multiplexed in large-scale, the sensing units based on balanced interferometers or the unbalanced interferometers (whose arm-length difference is about tens to hundreds of meters) with remote optical path matching technology are usually used to eliminate the adverse impact of the laser phase noise on the performance of fiber-optic hydrophone arrays [6], [7]. But the perfect path matching is not practical in the actual mass production, and the path matching for the fiber-optic hydrophone was usually controlled within about the level of 1∼2 mm [8].

OFDR technology is well-suited for the arm-length difference measurement of fiber interferometers, due to its measurement range of about tens to hundreds of meters, with spatial resolution of tens of microns and no dead zone [9], [10], [11]. However, it is usually assumed that the fiber interferometer under test is static, or unchanging, when OFDR is used [12]. Sometimes the environmental vibration and noise is inevitable during the time of measurement, and will generate the phase noise into the measured data from the interferometers. When the intensity of the phase noise related with the dynamic environment reaches a certain level, the beat frequency spectrum of the coherence signal from the interferometer will be broadened. This adverse impact will cause the resulting measurement greatly degraded, especially for the optical fiber interferometers with long arm length or the test arm wound on the elastomer, which is very sensitive to the environmental vibration and noise. Bos of Luna innovation company put forward a motion compensation method to removing adverse effects of motion in OFDR measurement [13], [14]. They used Rayleigh backscatter as the transducer to remove the adverse effects of motion, but this method is not suitable for the fiber interferometer with strong internal reflection [15].

In this paper, we present and demonstrate a novel method of environmental vibration and noise removing in OFDR measurements for the arm-length difference of optical fiber interferometer. Through a set of optical paths based on dual-laser coherent detection technology and the related ERPNS algorithm to extract the environmental phase noise from the measurement data to effectively reduce OFDR's sensitivity to vibration for the arm length difference measurement of the fiber interferometer in dynamic environment. The detail theoretical analysis is demonstrated and the validity of the ERPNS technology based on OFDR is verified experimentally.

II. Theoretical Analysis and Simulation

Fig. 1(a) shows the diagram of the arm length difference measurement of optical fiber interferometer based on the conventional OFDR technology. The measured interferometer

Manuscript received 19 September 2023; revised 20 November 2023; accepted 30 November 2023. Date of publication 5 December 2023; date of current version 26 December 2023. This work was supported in part by the National Key R&D Program of China under Grant 2023YFB2905300, in part by the Joint Project of National Natural Science Foundation of China under Grant U23A20379, in part by the 2023 Military Civilian Integration Project in Shanghai under Grant 23xtcx00500, and in part by the Shanghai Municipal "Science and Technology Innovation Action Plan" Social Development Science and Technology Breakthrough project under Grant 23DZ1203900. *(Corresponding authors: Lei Ye; Qing Ye.)*

The authors are with the Key Laboratory of Space Laser Communication and Detection Technology, Shanghai Institute of Optics and Fine Mechanics, Chinese Academy of Sciences, Shanghai 201800, China, and also with the Center of Materials Science and Optoelectronics Engineering, University of Chinese Academy of Sciences, Beijing 100049, China (e-mail: shuailuwei@siom.ac.cn; yelei@siom.ac.cn; yeqing@siom.ac.cn).

Digital Object Identifier 10.1109/JPHOT.2023.3339137

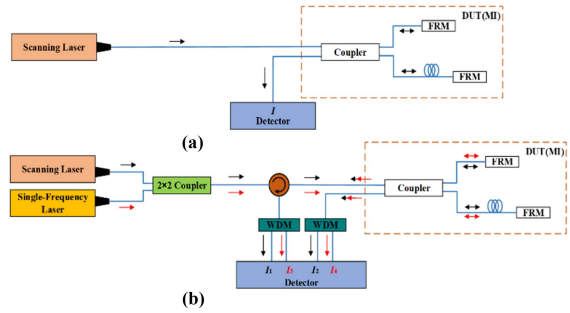

Fig. 1. Measurement of arm-length difference of fiber interferometer with (a) the conventional OFDR and (b) the OFDR with ERPNS technology.

is a Michelson interferometer (MI). The linear scanning light output from the scanning laser passes through a N × N coupler and enters into the reference arm and the measurement arm respectively. After reflected by the Faraday reflection mirrors (FRMs), the light transmitting in the two arms interferes at the output of the interferometer. If the MI is in static during the measurement, the arm length difference is a fixed value. Then the beat frequency of the coherent signal is linearly related to the time delay difference corresponding to the length difference between the measurement arm and the reference arm.

Supposing that the wavelength tuning rate of the scanning laser is linear in time, then the simple electric field expression *E(t)* of the output light is:

$$E\left(t\right) = E_0 e^{j2\pi f(t)t} \tag{1}$$

where E_0 is the amplitude of electric field amplitude $f(t) = f_0 + 0.5^{*}\gamma t$, f_0 is the initial optical frequency, γ is the wavelength tuning rate. The output interference signal in time domain can be expressed as:

$$I\left(t\right) \propto \cos\left(2\pi f_b t + 2\pi f_0 \tau - \pi\gamma\tau^2\right) \tag{2}$$

where the $f_b = \gamma\tau$ is the beat frequency of the interference signal and the $\tau = 2nL/c$ is the time delay difference corresponding to the arm-length difference L of the MI in the static state. Through a Fourier Transform, the interference signal in Formula (2) can be converted from time domain into frequency domain, and then a reflection peak at the beat frequency can be obtained with the optical path resolution of measurement $\Delta l_{\min}$

$$\Delta l_{\min} \cong \frac{\lambda^2}{2n\Delta\lambda} \tag{3}$$

where $\Delta\lambda$ is the scanning range of optical wavelength, λ can be the mid-value of optical wavelength of the scanning laser. Transform the Formula (2) to the frequency domain by a Fourier transform,

$$\mathcal{F}\left[I\left(t\right)\right] \propto \delta\left(f - f_b\right) e^{2\pi f_0\tau - \pi\gamma\tau^2} \tag{4}$$

Due to the linear relationship between the beat frequency and the time delay difference of the interferometry's two arms, the static arm-length difference $L = (f_b c)/(2n\gamma)$ can be easily obtained. However, if the interferometer is subjected to environmental disturbance, the Formula (2) is rewritten as

$$\begin{aligned} I(t) \propto \cos[&2\pi\gamma(\tau + \Delta\tau(t))t + 2\pi f_0\tau + 2\pi f_0\Delta\tau(t) \\ &- \pi\gamma\tau^2 - \pi\gamma\Delta\tau^2(t)] \end{aligned} \tag{5}$$

$$\begin{aligned} \Delta\tau(t) &= \left[\frac{-n}{c}\cdot\frac{(1-2v)}{Y} + \frac{1}{2}\cdot\frac{n^3}{c}\cdot\frac{(p_{11}+2p_{12})(1-2v)}{Y}\right]\cdot L\cdot P(t) \\ &= \xi\cdot L\cdot P(t) \end{aligned} \tag{6}$$

where $\Delta\tau(t)$ is the time-dependent delay function due to changes in both physical length and refractive index of the arm-length difference, not limited by the type of vibration, v is the Poisson ratio, p_{11} and p_{12} are the strain-optic coefficients, Y is the Young's modulus of the fibers, and *P(t)* is the stress applied to optical fiber at the time of t. For $\pi\gamma\tau^2 - \pi\gamma\Delta\tau^2(t) \approx 0$, then Formula (5) can be simplified as

$$I(t) \propto \cos\left[2\pi\gamma(\tau + \Delta\tau(t))t + 2\pi f_0\tau + 2\pi f_0\Delta\tau(t)\right] \tag{7}$$

It can be seen that the environmental random phase noise $2\pi\gamma\Delta\tau(t)t + 2\pi f_0\tau(t)$ is introduced into the output interference signal. According to the principle of OFDR, Fourier transform is often used to perform spectral analysis of signals to obtain τ. If the maximum variation of optical path is less than the optical path resolution of measurement, that is $|\Delta\tau(t)|_{\max} < 2n\Delta l_{\min}/c$, which represents approximate formula $\tau + \Delta\tau(t) \approx \tau$. So the Formula (7) can be further simplified as

$$I(t) \propto \cos\left[2\pi f_b t + 2\pi f_0\tau + 2\pi f_0\Delta\tau(t)\right] \tag{8}$$

On the other hand, when $|\Delta\tau(t)|_{\max} \geq 2n\Delta l_{\min}/c$, the corresponding signal in the frequency domain is widened due to environmental interference, and the width exceeds the spatial resolution of the system. The approximate formula is not satisfied, making it impossible to obtain accurate results τ. Therefore, the theory in the following needs to be satisfied $\tau + \Delta\tau(t) \approx \tau$.

Then, the phase term $2\pi f_0\Delta\tau(t)$ is the main factor affecting resulting measurement. It is assumed that the environmental vibration is a periodic sine signal, and the $\Delta\tau(t)$ can be expressed as

$$\Delta\tau\left(t\right) = |\Delta\tau(t)|_{\max}\sin\left(2\pi f_m t\right) \tag{9}$$

where f_m is the fiber vibration frequency. The Bessel expansion of (8) is

$$\begin{aligned} I(t) \propto &\cos\left[2\pi\left(f_b t + f_0\tau\right)\right] \\ &\cdot\left\{J_0(z) + 2\sum_{n=1}^{\infty} J_{2n}(z)\cos\left(2n\cdot 2\pi f_m t\right)\right\} \\ &- \sin\left[2\pi\left(f_b t + f_0\tau\right)\right] \\ &\cdot\left\{2\sum_{n=1}^{\infty} J_{2n-1}(z)\sin\left[(2n-1)\cdot 2\pi f_m t\right]\right\} \end{aligned} \tag{10}$$

where the vibration modulation depth $z = 2\pi f_0|\Delta\tau(t)|_{\max}$ which may be determined by the Formula (6) and the mechanical parameters of the optical fiber, represents OFDR's sensitivity to environmental vibration. The related one-sided spectral function is

$$\begin{aligned} I^{(1)}(f) \propto e^{j2\pi f_0\tau}\cdot\{&J_0(z)\delta\left(f - f_b\right) \\ &+ \sum_{n=1}^{\infty} J_{2n}(z)\cdot\left[\delta\left(f - f_b - 2nf_m\right) + \delta\left(f - f_b + 2nf_m\right)\right] \end{aligned}$$

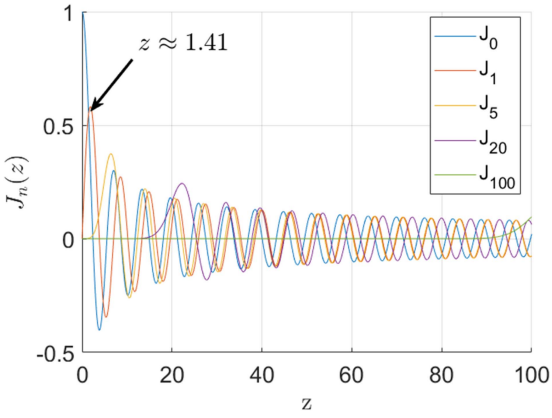

Fig. 2. Bessel function.

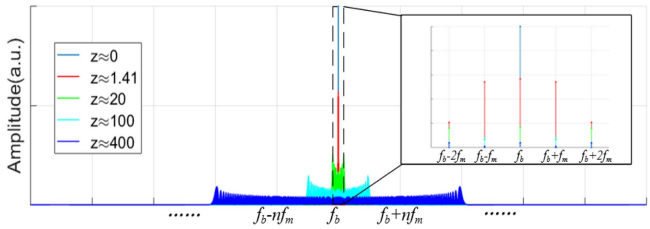

Fig. 3. Beat frequency and its harmonic components with different z.

$$+\sum_{n=1}^{\infty} J_{2n-1}(z)\cdot[-\delta(f-f_b-(2n-1)f_m) + \delta(f-f_b+(2n-1)f_m)]\} \quad (11)$$

From the Formula (11), it can be seen that the vibration will broaden the beat frequency spectrum by introducing harmonic components related with f_m around the location of the beat frequency. Fig. 2 shows the first three order Bessel functions. When $z < 1.41$, $J_0(z)$ is always higher than $J_n(z)$. In this case, the beat frequency f_b can be obtained by finding the highest reflection peak in frequency domain, with the effect of the environmental vibration when $|\Delta\tau(t)|_{\max} < 2n\Delta l_{\min}/c$. But this simple method is no longer suitable for the situation that the reflection peak related with the beat frequency f_b may not be the highest one, when $z > 1.41$, seen in Fig. 3.

To obtain the accurate static arm-length difference L of the interferometer, an ERPNS technology is proposed. Based on OFDR technology, a single-frequency laser is used to obtain the interference signal whose phase term does not include the beat frequency information. The related ERPNS algorithm is developed to extract the environmental phase noise from the measurement data by utilizing the fixed phase difference between the two arbitrary outputs of a N × N fiber coupler with a WDM method. This ERPNS technology can be used to reduce OFDR's sensitivity to vibration for the arm length difference measurement of the fiber interferometer. The related scheme is shown in Fig. 1(b). The light output from the scanning laser and the single-frequency laser is combined by a 2 × 2 optical fiber coupler and then enters the MI under test through a circulator. The two optical interference signals with fixed phase difference are output from the MI, one directly goes into a WDM, when another one goes into a WDM through the circulator. And the optical beams are split by the two WDMs respectively into the optical interference signals, I_1 and I_2, whose wavelengths are corresponding to the scanning laser, and the optical interference signals, I_3 and I_4, whose wavelengths are corresponding to the single-frequency laser. These interference signals can be expressed as

$$I_1 \propto \cos\left[2\pi f_b t + 2\pi f_{10}\tau + 2\pi f_{10}\Delta\tau(t) - \frac{\alpha}{2}\right] \quad (12)$$

$$I_2 \propto \cos\left[2\pi f_b t + 2\pi f_{10}\tau + 2\pi f_{10}\Delta\tau(t) + \frac{\alpha}{2}\right] \quad (13)$$

$$I_3 \propto \cos\left[2\pi f_{20}\tau + 2\pi f_{20}\Delta\tau(t) - \frac{\alpha}{2}\right] \quad (14)$$

$$I_4 \propto \cos\left[2\pi f_{20}\tau + 2\pi f_{20}\Delta\tau(t) + \frac{\alpha}{2}\right] \quad (15)$$

where α is the fixed phase difference between the two outputs of the N × N coupler, f_{10} is the initial optical frequency of the scanning laser and f_{20} is the central optical frequency of the single-frequency laser. Then, the difference value *D(t)* can be obtained by the subtraction operation between the product value of the Formula (12) and the Formula (15), and the product value of the Formula (13) and the Formula (14) as

$$D(t) \propto \sin\alpha \cdot \sin\left[2\pi f_b t + 2\pi\Delta f\tau + 2\pi\Delta f\cdot\Delta\tau(t)\right] \quad (16)$$

where the frequency difference $\Delta f = f_{10} - f_{20}$. In the Formula (8), the vibration modulation depth z turns to be $2\pi\Delta f|\Delta\tau(t)|_{\max}$, which means the sensitivity of OFDR to environmental vibration is decreased by $20\log(f_0/\Delta f)$ in comparison with the Formula (8). When $\Delta f = 0$,

$$D(t) \propto \sin(\alpha)\sin\left[2\pi f_b t\right] \quad (17)$$

then the static arm-length difference L of the optical fiber interferometer can be obtained ideally in dynamic environment. Fig. 4(a), (b) and (c) show the location maps of the reflection peak compared with two algorithms in theoretical simulation. The figure shows that ERPNS technology can effectively reduce the environmental vibration in theoretical simulation.

III. Experiment

In order to verify the validity of the ERPNS technology based on OFDR in dynamic state, an experimental system is setup, as shown in Fig. 5. In Section II, the Formula (17) shows that the proposed method can completely eliminate environmental interference when $\Delta f = 0$. Therefore, the closer the center wavelength of a single frequency laser is to the initial wavelength of a scanning frequency laser, the better the method can remove the interference of environmental noise on the results. Moreover, the central wavelength of the WDM should be the same as possible with the initial wavelength of the scanning laser, and the bandwidth of the WDM needs to be narrow enough under the condition of meeting the scanning range. In our experiment, an external cavity tunable laser (Luna phoenix 1200) with a linewidth of about 1.5 MHz, wavelength scanning range of 1549.5∼1564.5 nm (∼56 μm spatial resolution, the initial wavelength 1549.5 nm is identified by the synchronization

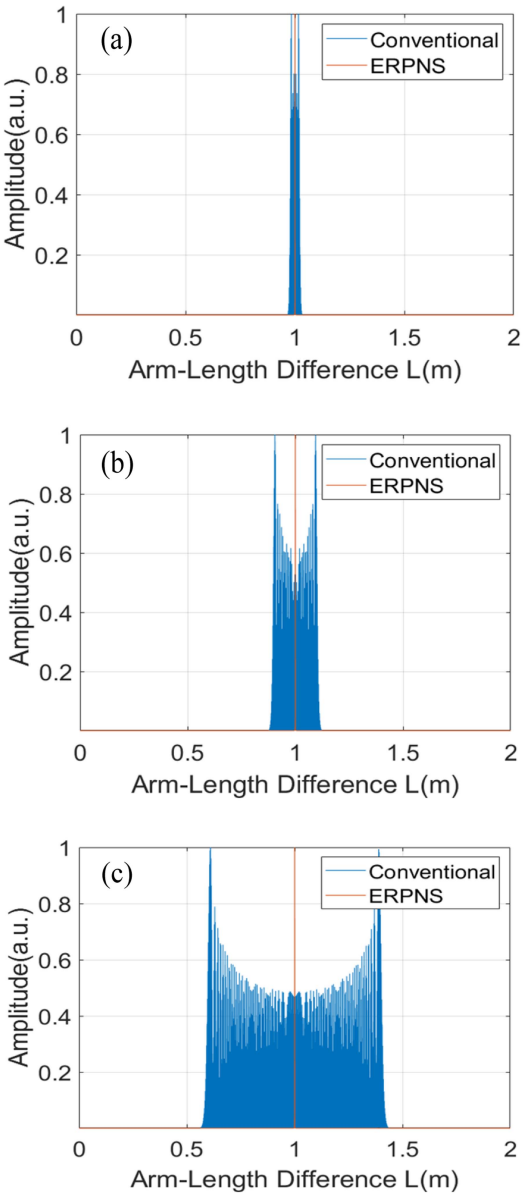

Fig. 4 Location map of the reflection peak with the vibration modulation in theoretical simulation with (a) z = 20, (b) z = 100, and (c) z = 400.

signal output by the laser itself) and tunable rate of 40 nm/s is used as the scanning laser source. A planar external cavity low-noise laser (RIO ORIONTM laser module) with very stable central wavelength of about 1548.5 nm is used as the single-frequency laser source. In this experiment, a reference interferometer with arm length difference of about 150 m is added to produce an optical interference signal to resample *D(t)* for eliminating the adverse influence of actual nonlinear scanning [16]. The related the maximum detectable distance of the system is about 75 m. The central wavelength of the WDM is about 1548.5 nm, with bandwidth of about 1 nm (the sensitivity of OFDR to environmental vibration decreases by ∼60 dB in theory). All the optical interference signals from the DUT and the reference interferometer are detected by five photodetectors (PD, Newport, 1811). Due to the highest frequency of reference

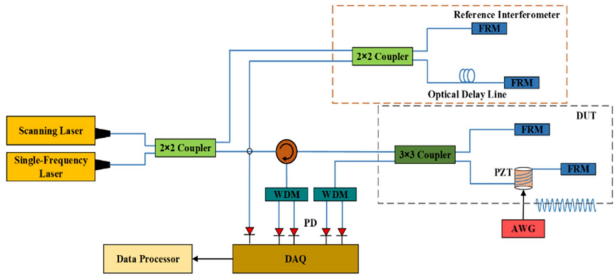

Fig. 5. Experiment setup.

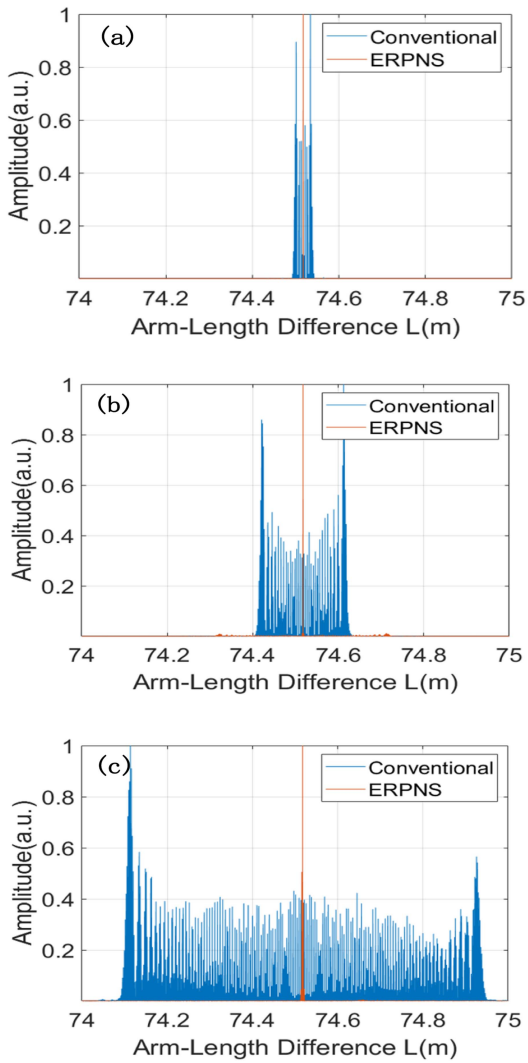

Fig. 6. When fm = 100 Hz, the location map of the reflection peak with the vibration modulation depth z of about (a) z = 20, (b) z = 100, and (c) z = 400, respectively.

interferometer's output signal being about 12 MHz, the sampling rate of the data acquisition card (DAQ) is 60 MS/s, meeting the requirements. In data processing, according to ERPNS technology, the data related to Formulas (12)–(15) is calculated as the data related to Formula (17), and then resampled using the reference interferometer signal. At this point, the sensitivity of environmental interference has decreased by ∼60 dB, and after

TABLE I
STATIC ARM-LENGTH DIFFERENCE L AT DIFFERENT VIBRATION MODULATION DEPTH z, WHEN $F_{\mathrm{m}} = 100$ HZ

z	20 m	100m	400m
CON 1	74.519014	74.518991	74.519004
CON 2	74.518989	74.518993	74.519001
CON 3	74.519014	74.519047	74.519029
CON 4	74.519015	74.519019	74.519001
CON 5	74.519015	74.519015	74.519001
CON 6	74.518986	74.519018	74.519027
CON 7	74.519042	74.519018	74.519000
CON 8	74.519042	74.519019	74.519028
CON 9	74.519015	74.519016	74.519030
CON 10	74.519015	74.519019	74.519028
Mean Value (m)	74.519015	74.519015	74.519015
Error Value (m)	-0.000029	0.000031	0.000015

resampling, it will not affect the measurement results. The DUT is a Michelson interferometer mainly made of two FRMs, a 3×3 coupler and a piezoelectric transducer (PZT), with about $2/3\pi$ difference phase difference between the two outputs of the MI and arm length difference of 74.51902 m measured by the conventional OFDR in the state with the ambient noise is about 47.2 dBA (the related $c \cdot |\Delta\tau(t)|_{\max}$ is about 6.6×10^{-13} m, which is far less than the optical path resolution of the system), and the ambient temperature of 25±0.5 °C. A PZT acts as a vibration source which introduces the variation $\Delta\tau(t)$ into the arm-length difference of the MI, and the vibration amplitude and frequency can be controlled by a function generator (WF1974).

Although not limited by the type of vibration, to make quantitative analysis of the effect of the ERPNS technology, here, a sinusoidal wave with fixed frequency of 100 Hz is added on the PZT as vibration signals. By changing the voltage of the signals, the vibration modulation z will be set by about 20, 100, 400 respectively.

In experiment, by adjusting the maximum variation of the physical length of the fiber around the PZT, the actual z is easily obtained by $z = 2\pi f_0 |\Delta\tau(t)|_{\max}$. Fig. 6(a), (b), and (c) show the location maps of the reflection peak related with the static arm-length difference L obtained through the conventional OFDR and the ERPNS technology based on OFDR with the vibration modulation depth z of about 20, 100, and 400 respectively, when the frequency of the vibration source put on the interferometer f_m is 100 Hz. In each figure after dealt by ERPNS, the highest reflection peak related with the static arm-length difference L can been obviously, with OFDR's sensitivity to vibration is decreased effectively in dynamic environment. This is the same conclusion as the theoretical simulation experiment.

Table I shows the test results of the static arm-length difference L for 10 times with the vibration modulation depth z of about 20, 100, and 400 respectively. The results are presented in Table I, the error value in different measurement condition is less than ∼0.03 mm.

IV. CONCLUSION

An ERPNS technology based on OFDR is present and demonstrated to extract the environmental phase noise from the measurement data to rise the measurement ability of OFDR for the static arm length difference measurement of optical fiber interferometers in dynamic environment, when the maximum variation of optical path is less than the optical path resolution of the system. Our preliminary experiment achieves a measurement accuracy better than 0.05 mm for the static arm length difference of 74.51902 m in different dynamic environment by decreasing OFDR's sensitivity to vibration by ∼60 dB in theory, with 56 μm of spatial resolution in the maximum detectable distance of about 75 m. These results demonstrate the potential of the ERPNS technology based on OFDR used for accurate, high-spatial resolution measurement of the static arm length difference for optical interferometers in dynamic environment.

REFERENCES

[1] K. S. Sham et al., "Experimental investigations on implementing different PGC algorithms for interrogation of fiber optic hydrophones," *Proc. SPIE*, vol. 9654, pp. 463–470, 2015.

[2] M. Y. Plotnikov, V. S. Lavrov, P. Y. Dmitraschenko, A. V. Kulikov, and I. K. Meshkovskiy, "Thin cable fiber-optic hydrophone array for passive acoustic surveillance applications," *IEEE Sensors J.*, vol. 19, no. 9, pp. 3376–3382, May 2019, doi: 10.1109/JSEN.2019.2894323.

[3] Y. Cai et al., "Noise reduction with adaptive filtering scheme on interferometric fiber optic hydrophone," *Optik*, vol. 211, 2020, Art. no. 164648, doi: 10.1016/j.ijleo.2020. 164648.

[4] W. Xiong et al., "Sensitivity enhanced fiber optic hydrophone based on an extrinsic Fabry-Perot interferometer for low-frequency underwater acoustic sensing," *Opt. Exp.*, vol. 30, pp. 9307–9320, 2022, doi: 10.1364/OE.451678.

[5] A. Dandridge and A. B. Tveten, "Phase noise of single-mode diode lasers in interferometer systems," *Appl. Phys. Lett.*, vol. 39, pp. 530–532, 1981.

[6] A. D. Kersey and A. Dandridge, "Phase-noise reduction in coherence-multiplexed interferometric fiber sensors," *Electron. Lett.*, vol. 22, pp. 616–618, 1986.

[7] C. Cao, Z. Hu, S. Xiong, and Y. Hu, "Transmission-link-induced intensity and phase noise in a 400-km interrogated fiber-optics hydrophone system using a phase-generated carrier scheme," *Proc. SPIE*, vol. 52, 2013, Art. no. 096101, doi: 10.1117/1.OE.52.9.096101.

[8] C. K. Kirkendall and A. Dandridge, "Overview of high performance fibre-optic sensing," *J. Phys. D Appl. Phys.*, vol. 37, pp. 197–216, 2004, doi: 10.1109/CLEO.2002.1034123.

[9] Z. Zhang, X. Fan, M. Wu, and Z. He, "Phase-noise-compensated OFDR realized using hardware-adaptive algorithm for real-time processing," *J. Lightw. Technol.*, vol. 37, no. 11, pp. 2634–2640, Jun. 2019, doi: 10.1109/JLT.2018.2875210.

[10] Z. Yao, T. Mauldin, Z. Xu, G. Hefferman, and T. Wei, "An integrated OFDR system using combined swept-laser linearization and phase error compensation," *IEEE Trans. Instrum. Meas.*, vol. 70, 2021, Art. no. 7000208, doi: 10.1109/TIM.2020.3011485.

[11] X. Zhang et al., "Characterizing microring resonators using optical frequency domain reflectometry," *Opt. Lett.*, vol. 46, pp. 2400–2403, 2021, doi: 10.1364/OL.425681.

[12] M. E. Froggatt et al., "Method and apparatus for motion compensation in interferometric sensing systems," U.S. Patent 11193751B2, Dec. 07, 2021.

[13] J. J. Bos and N. A. Rahim, "Motion compensation in distributed fiber optic sensing via optical frequency domain reflectometry," *Proc. SPIE*, vol. 9157, pp. 817–820, 2014, doi: 10.1117/12.2058789.

[14] S. T. Kreger, J. W. Klein, N. A. A. Rahim, and J. J. Bos, "Distributed Rayleigh scatter dynamic strain sensing above the scan rate with optical frequency domain reflectometry," *Proc. SPIE*, vol. 9480, pp. 25–31, 2015, doi: 10.1117/12.2177578.

[15] M. A. S. Zaghloul et al., "High spatial resolution radiation detection using distributed fiber sensing technique," *IEEE Trans. Nucl. Sci.*, vol. 64, no. 9, pp. 2569–2577, Sep. 2017, doi: 10.1109/TNS. 2017.2735546.

[16] M. E. Froggatt, D. K. Gifford, S. Kreger, M. Wolfe, and B. J. Soller, "Characterization of polarization-maintaining fiber using high-sensitivity optical-frequency-domain reflectometry," *J. Lightw. Technol.*, vol. 24, no. 11, pp. 4149–4154, Nov. 2006, doi: 10.1109/JLT.2006. 883607.